Tectonophysics 633 (2014) 126–142

Contents lists available at ScienceDirect

Tectonophysics

journal homepage: www.elsevier.com/locate/tecto

The engines of gravity-driven movement on passive margins: Quantifying the relative contribution of spreading vs. gravity sliding mechanisms

Frank J. Peel *

National Oceanography Centre, University of Southampton Waterfront Campus, European Way, Southampton SO14 3ZH, United Kingdom

ARTICLE INFO

Article history:
Received 24 January 2014
Received in revised form 20 June 2014
Accepted 22 June 2014
Available online 30 June 2014

Keywords:
Gravity tectonics
Gravity spreading
Gravity gliding
Passive margin deformation
Angola
Orange Basin

ABSTRACT

Movement of gravity-driven systems on passive margins is fuelled by the loss of gravitational potential energy. Two end-member modes (gravity spreading and gravity gliding) are defined by whether the potential energy loss is due to deformation and movement towards the base of the system (spreading), or by movement parallel to the base of the system (gliding); most natural systems consist of a mixture of the two processes.

Hitherto, use of these concepts has been limited or equivocal due to lack of a quantitative measure. In some cases, characterisation of gliding vs. spreading systems based on secondary attributes has resulted in controversy, because there is a lack of consensus as to which of these are truly diagnostic. This paper presents a new, simple quantitative method based on vector analysis, providing a numerical measure of the relative contribution of spreading vs. gliding. The method is applied to synthetic examples, where deformation can be tracked, and to natural examples where a valid palinspastic reconstruction is available. The results confirm that most natural examples exhibit mixed-mode behaviour, and that some have been mischaracterized; much of the Angola margin is dominated by spreading. The method can also provide an estimate of the absolute amount of gravitational potential energy released in the movement, and the energy contribution made by gliding vs. spreading. Determining the dominant process has implications for predicting the development of seafloor topography and stratal architecture.

1. Introduction

Deformation of sedimentary sequences by gravity-driven tectonics occurs in most of the world's passive margins (Morley et al., 2011; Rowan et al., 2004) and also in other planets (Montgomery et al., 2009). Gravity-driven deformation commonly consists of thin-skinned linked systems, in which a body of sediments is translated basinwards, accommodated by extension in its updip portion, and contraction in the downdip region. This can occur on a range of scales, from small failures effecting a few metres of sediment (e.g. Alsop and Marco, 2013) to giant systems affecting bodies 10s of km thick and 100s of km long in the transport direction (e.g. Peel et al., 1995). These systems are economically important: they create structures containing substantial hydrocarbon resources (e.g. Moore, 2010). In some ways we now understand these systems very well; modern seismic data reveals their architecture; well penetrations constrain the lithology and age of the sediment sequences; sequential structural restorations reveal how the geometries we see today evolved through time. We know how the systems are powered, in a general sense: the energy source is the gravitational potential of the sediments. Energy is released as the sediments move downwards, and this powers the lateral movement and deformation. A gravitationally driven linked system from the Orange Basin margin of South Africa (Fig. 1) illustrates this principle, showing a clear separation of the updip extensional region from the downdip contractional portion. It is obvious that material has moved downwards, providing the energy that fuels the system. It is also clear that the "engine" which converts this energy into movement is complex; downward movement of sediments is achieved both by movement on the basal slip surface and by internal deformation within the body of the linked system. These two components correspond to the processes known as gravity gliding and gravity spreading, respectively (Ramberg, 1967, 1977, 1981a,b).

Distinguishing the relative contribution of gliding vs. spreading could contribute significantly to our understanding of gravity-driven systems. For example, this may determine the extent to which movement is related to sediment input to the margin, and thus whether the movement is continuous or episodic. It may determine what the rate-limiting factors are, and thus control the rate of movement. It has been suggested that both the location and the direction of propagation of the contractional toe region may be different in gliding vs. spreading systems (Brun and Fort, 2011). Rowan et al. (2000, 2004) proposed that the transition from early systems dominated by gravity gliding to younger systems dominated by gravity spreading may be an important component of the evolution of margins such us the northern Gulf of Mexico.

* Tel.: +44 2380 596562.
E-mail address: Frank.peel@noc.ac.uk.

http://dx.doi.org/10.1016/j.tecto.2014.06.023

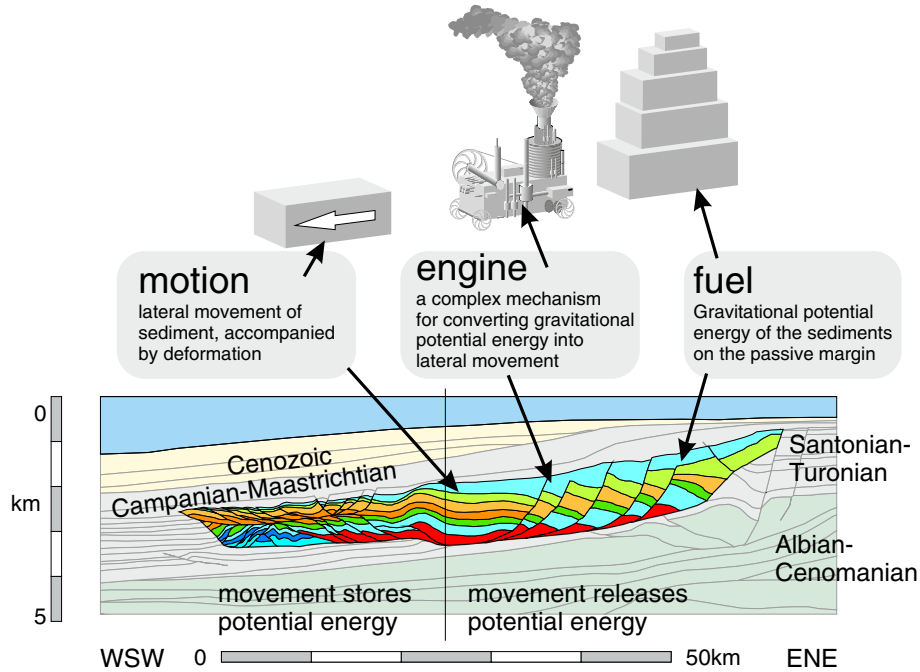

Fig. 1. A gravity-driven linked system in Upper Cretaceous sediments of the Orange Basin, South Africa, interpreted by the author. Section is in depth with 5:1 vertical exaggeration. Interpretation is based on 2D seismic reflection data; the horizons shown are correlated seismic horizons, whose precise age is not known. The gross stratigraphic correlation follows that of Brown et al. (1995) and de Vera et al. (2010).

However, in many real-world examples it can be difficult to characterize deformation as gliding-dominated or spreading-dominated using qualitative methods (Schultz-Ela, 2001), and thus our ability to characterize passive-margin deformation in these terms is limited and potentially confused, and their use has fallen out of favour.

This paper sets out a new and simple quantitative method for estimating the relative contribution of gliding vs. spreading, based on a return to the original definition of the terms. This method uses simple geometric analysis of the net movement vectors, obtained by comparing a present-day cross section with structural restorations, to determine where the energy driving the system comes from, and this alone is sufficient to characterize the amount of gliding vs. spreading. The method is generally applicable, since it is concerned only with the gross kinematics of the system and is irrespective of the lithology, rheology, fluid pressure or any of the many other factors that control the form and detailed expression of the final structure.

The method is applicable to large-scale (>1 km thickness), slow-moving systems in which kinetic energy is negligible, and is not designed for fast, catastrophic systems in which kinetic energy is significant.

2. The definition of gravity spreading and gravity gliding

2.1. The original definitions of gravity spreading and gravity gliding in mountain belts

The concepts of gravity tectonics were developed to provide a mechanism for large-scale lateral movement seen in mountain belts (e.g. Bucher, 1956; Elliott, 1976; Kehle, 1970; van Bemmelen, 1960, 1965) and the coexistence of extension and contraction in orogenic complexes (Platt, 1986).

De Jong and Scholten (1973) and Ramberg (1967, 1977, 1981a,b) defined two distinct modes of gravity-driven deformation: gravity gliding (a.k.a. gravity sliding) and gravity spreading. Ramberg (1981a) explicitly defined these terms based on the manner in which gravitational potential energy is decreased by the movement. The key words from this defining paper are reproduced here to emphasize the significance of energy to the definition: "Within most orogens … three types of structures can be distinguished; … diapirs, … nappes spread plastically over their substratum and … rock masses which have slid down inclined surfaces. These are phenomena whose immediate cause — that is, immediate driving energy — is found in the orogenic architecture itself. The structures mentioned are the results of the dissipation of gravity potential on a regional or local scale.... the energy behind the vertical sagging and complementary horizontal spreading recorded in some nappes is also a decreasing energy potential. When a nappe thins, its centre of gravity descends. That is equivalent to saying that the gravity potential of the nappe decreases as it moves. In contrast to a plastically collapsing nappe, a rock-mass sliding down an inclined surface may exhibit no … internal sagging or plastic collapse. The rock may move as a rigid unit. Again, it is evident that the gravity potential decreases during the slide". This is made clear in the original illustrations (Fig. 2a–b).

We may restate this more simply: in gravity spreading, the energy is released by lowering of the centre of gravity due to thinning of the material. In gravity gliding, the energy is released by lowering of the centre of gravity due to movement along an inclined surface. This consideration alone is sufficient to define the terms in a manner entirely consistent with the original intention.

This return to the original intention also clarifies two other potential sources of confusion. Gliding vs. spreading are not defined either by rigidity, or by whether there is block movement. In pure gliding, the moving unit may act as a rigid block, but it may equally well experience significant internal shearing (Brun and Merle, 1985), and viscous material may also be described as gliding (Kehle, 1970), as long as movement is parallel to the base of the unit, and the base is dipping. Conversely, a spreading system may consist of multiple rigid blocks (Schultz-Ela, 2001). Of necessity, there is a component of movement parallel to the base of the unit in both gliding and spreading modes, as clearly shown in Fig. 2a–b. It is not whether there is base-parallel movement that matters, but whether that movement releases energy. In Fig. 2a, the movement parallel to the base releases gravitational potential energy; in Fig. 2b, movement parallel to the base does not release energy.

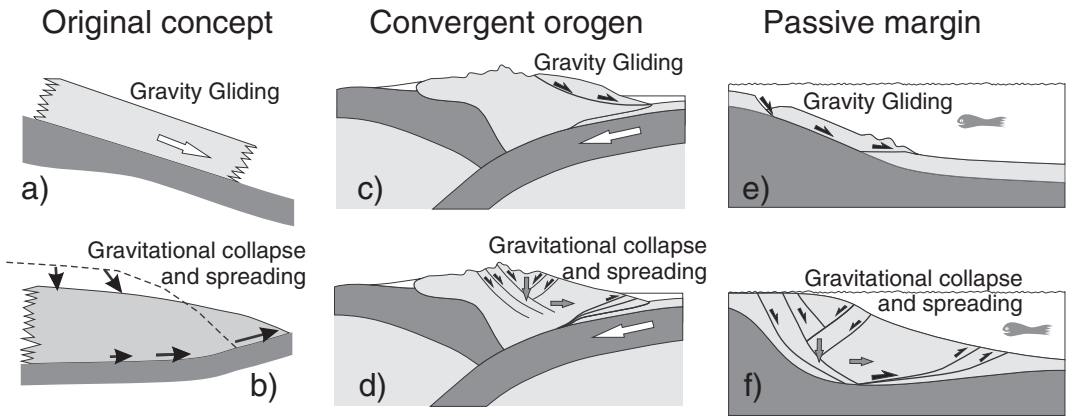

Fig. 2. The concepts of gravity gliding and gravity spreading. a, b: original concept. c, d: as applied to a convergent orogenic belt. e, f: applied to a passive margin setting. a, b: redrawn from Ramberg (1981a); c, d: after Rey et al. (2001), Platt, 1986; e, f: after Morley et al. (2011).

This definition of gravity spreading vs. gravity gliding depends on the source of the energy, specifically whether it is released by movement parallel to the base (gliding) or by movement perpendicular to the base (spreading). The definition does not specify the lithology of the unit, nor its rheology (ductile, brittle, viscous, or plastic — except that gravity spreading requires deformation of some sort and therefore it cannot be a single rigid block), nor the angle of dip of the top of the unit, nor whether the unit is deforming by homogeneous or inhomogeneous strain, nor whether the deformation is distributed vs. localized (e.g. by faulting). There is a common association of some of these factors with spreading or sliding modes, but it is important to note that the definition does not depend on them.

The definition of gliding vs. spreading depends specifically on the manner in which gravitational potential energy is released, and therefore is determined by examining only the part of the system that releases energy (generally the extensional heel/updip portion of a linked system). While it is also worthwhile considering the energy balance of the entire system, because this reveals much about how the system works, this article is focussed on the specific issue of quantifying gliding vs. spreading, and its implications. As a result the analyses presented here are focussed on the energy-releasing part of the system (e.g. the right hand portion of Fig. 1).

2.2. Application to other tectonic settings

The original concepts of gravity tectonics in orogenic belts were created to explain the significant lateral movement seen in mountain belts. However, their perceived importance in that setting has diminished as the dominant role of lateral contraction driven by plate convergence has been recognized. Regions within mountain belts formerly interpreted as classic examples of gravity gliding tectonics, such as the Subalpine Chains of south-eastern France (Fallot and Faure-Muret, 1949) have been reinterpreted as thin-skinned thrust systems rooting into large-scale basement contraction (e.g. Bellahsen et al., 2012; Butler, 1986, 2013; Deville and Chauvière, 2000; Phillippe et al., 1998). Platt (1986) developed a hybrid model for orogenic belts in which gravity spreading is seen as a process which modifies an orogeny created by plate convergence (Fig. 2d).

However, although written with orogenic deformation in mind, the definitions of gravity tectonics apply in any tectonic setting (Rey et al., 2001), and are especially appropriate to the deformation of passive margins (Fig. 2e, f), where all movements are gravity-driven because there is no component of basement contraction.

2.3. Alternate definitions, terminology and attempts at diagnostic analysis

There is partial overlap of the definitions of gravity gliding and gravity spreading originating from consideration of orogenic processes on the large scale (as described above) with a similar suite of terms which have developed somewhat independently in the literature related to landslides. Cruden and Varnes (1996) and Varnes (1978) defined the terms "lateral spreading" and "sliding" for landslides, which are similar but not identical to the definition of gravity spreading and gravity gliding established for orogens by Ramberg (1967, 1977, 1981a,b). Their definitions[1] mix the geometric description (which is similar to that of Ramberg, 1967, 1977, 1981a,b) with associated observations (which depend on the specific rheology or lithology of materials commonly seen in landslides).

This paper follows the stricter definition and terminology of Ramberg (1967, 1977, 1981a,b).

Prior to this publication, there has been no quantitative method for distinguishing the contribution of spreading vs. gliding, and in lieu of this, a set of associated observations are commonly used to define which is the dominant process. Characterisation based on qualitative considerations alone appears to be equivocal, such that a well-studied margin such as the Northern Gulf of Mexico during the Cenozoic is described by some workers as a gravity-spreading-dominated system (Rowan et al., 2012; Worrall and Snelson, 1989) and by others as a gravity-gliding dominated margin (Brun and Fort, 2011). This confusion arises in part from a lack of consensus on the associated observations taken to be diagnostic of either mode.

Several authors have suggested lists of secondary structural observations which might be diagnostic of spreading or gliding (e.g. Brun and Fort, 2011; Schack Pedersen, 1987); but these lists are not consistent, nor are they universally accepted (Rowan et al., 2012). This paper takes no position on these proposed diagnostic associations, instead establishing an alternate method for defining spreading vs. gliding based on the source of the energy. Agreement on a common suite of associated diagnostic observations can be better achieved once we can specify which natural examples fall into which category.

[1] The following definitions from the landslide literature illustrate the mixture of process and associated observations. "Spreading is defined as an extension of a cohesive soil or rock mass combined with a general subsidence of the fractured mass of cohesive material into softer underlying material." (Cruden and Varnes, 1996); "in spreading, the dominant mode of movement is lateral extension accommodated by shear or tensile fractures" (Varnes, 1978), "sliding is downslope movement of a soil or rock mass occurring dominantly on the surface of rupture or on relatively thin zones of intense shear strain." (Cruden and Varnes, 1996).

The principal cause of confusion appears to stem from the fact that very few natural examples fall neatly into either end-member category: most examples exhibit mixed-mode behaviour, for which there is no established diagnostic method based on associated observations. Rowan et al. (2004) showed, as illustrated in Fig. 3, that the gliding and spreading modes represent end-member cases on a spectrum. Naturally occurring systems are commonly a mixture of the two. Pure gravity gliding (Fig. 3a) is a special case, only achievable if the translating block experiences no stretching and all movement is parallel to the base; this is rarely seen in nature. Pure spreading (Fig. 3b) is another special case, only achievable when the base of the system is perfectly horizontal, so that no energy is gained or lost by lateral movement: again this is rarely (if ever) seen. Note that if the basal decollement dips upwards in the transport direction, there will be an energy effect of the gliding component, but this will be negative (energy absorbed as stored potential energy). Almost all natural examples are a mixture, involving some spreading and some gliding component (Fig. 3c).

A secondary potential cause of confusion is that some systems may change in character with time. On the large scale, the Mississippi Fan Fold Belt of the Gulf of Mexico may have begun life as the toe of a gliding-dominant system, later transitioning to a spreading-dominant system (see Fig. 6 of Rowan et al., 2004). On the small scale, landslides which propagate by spreading-dominant processes may transition into gliding-dominant systems.

3. A quantitative method for determining the relative contribution of gliding vs. spreading

3.1. Quantifying the relative energy release for an idealized system

In pure gravity gliding (Fig. 4a), net movement is parallel to the base of the moving unit. All gravitational potential energy release results from the vertical component of this movement. Pure gliding permits, but does not require, shape change, as long as the net movement is parallel to the base of the unit.

The energy released by this movement (i.e. the change in gravitational potential energy, ΔP), is

$$\Delta P = Wn \sin\Theta$$

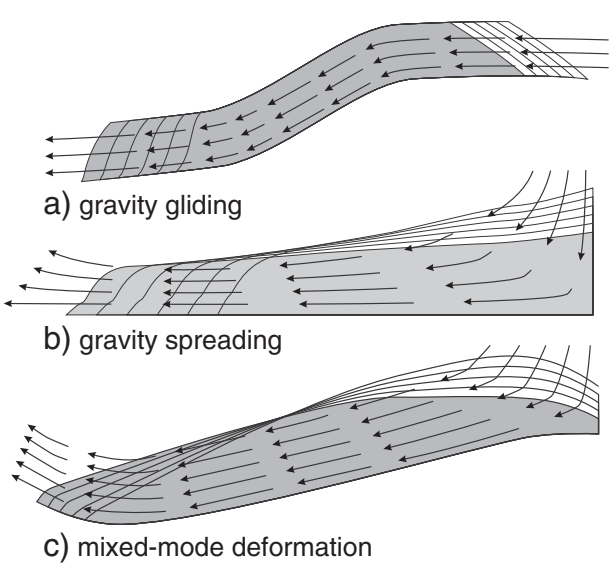

Fig. 3. End-member deformation modes for gravity gliding (a), gravity spreading (b) and a mixed mode case (c). Arrows show particle paths (Ramberg, 1975): successive positions of the body are shown by ghost lines.
Modified from Rowan et al. (2004).

where W is the effective weight of the block, corrected to account for any buoyancy effect,[2] n is the net movement of the centre of mass, and Θ is the angle of downwards dip of the basal slip surface in the transport direction.

Gravity spreading (Fig. 4b) relates to shape change of the unit. In gravity spreading, the movement that releases gravitational potential energy is the motion of the centre of gravity of the unit relative to its base, accommodated by deformation of the unit. All gravity spreading systems (even pure spreading systems) have a component of movement parallel to the basal surface.

In a pure spreading system, the base is horizontal, and the energy released by the movement is

$$\Delta P = Wn \sin\Phi$$

where n is the net movement of the centre of mass, and Φ is the angle between the movement of the centre of mass and the base of the system. Note that although there is a component of movement parallel to the base, this results in no vertical movement and hence it makes no energy contribution.

In a mixed-mode case (Fig. 4c), the base is inclined and there is internal deformation, and both components result in the release of potential energy. This can be resolved into $\Delta PE_{(spread)}$, the potential energy released by the spreading component ($\Delta PE_{(spread)} = Wn \sin\Phi \cos\Theta$) and $\Delta PE_{(glide)}$, the energy released by the gliding component ($\Delta PE_{(glide)} = Wn \cos\Phi \sin\Theta$). Following the original definitions of Ramberg (1967, 1977, 1981a,b), which are keyed to the source of the energy, we can use this simple analysis to characterize where a mixed-mode system falls on the spectrum between gliding and spreading on the basis of the relative contribution of these to the energy supply.

We can derive two simple measures of the relative contribution of spreading vs. gliding by combining these two functions:

The ratio of the energy supplied by spreading vs. gliding, $\Delta PE_{(spread)}/\Delta PE_{(glide)} = \tan\Phi/\tan\Theta$; and
α = Proportion of total energy contributed by spreading = $1/(1 + \tan\Phi/\tan\Theta)$.

These measures, which are sufficient to define where a system lies on the spectrum of spreading vs. gliding, depend only on the two angles Φ and Θ.

3.2. Variation of driving force with distance moved

Why is it important to understand the power supply of gravity failure in these terms? One important consequence is illustrated in Fig. 5. Movement in either a spreading or a gliding system decreases the gravitational potential energy, but in a gliding system the energy released per unit distance of displacement may remain constant (Fig. 5c), as long as it is moving down a uniform slope. By contrast, in a spreading-dominant system, the energy released per unit of displacement necessarily diminishes as displacement increases (Fig. 5d), unless the system is refuelled by the addition of more materials.

The total energy release is equivalent to the driving force multiplied by the distance of offset. We can therefore simply derive the total gross lateral driving force from the energy release and the lateral displacement. This is true regardless of how the energy is dissipated; the mechanisms of energy dissipation may be different in the gliding vs. spreading cases.

In consequence, the driving force of a gliding system in which the basal slope is constant should not change with increasing offset. By contrast, the driving force for a spreading system will progressively decrease with offset unless the engine of deformation is refuelled: in this case, the fuel is the gravitational potential of the sediments,

[2] For extraterrestrial examples, the weight is also adjusted to account for local gravity.

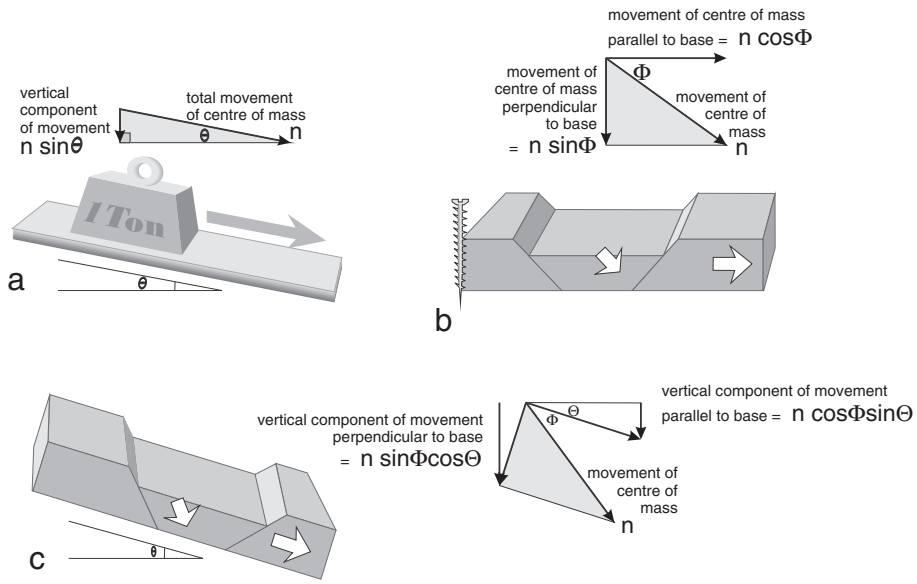

Fig. 4. Definition of gravity gliding (a) and gravity spreading (b) in terms of the energy-releasing movement, and quantification of the mixed-mode case (c). The angle Θ is the dip of the base of the system, and the angle Φ measures the angle between the movement of the centre of mass and the base of the system.

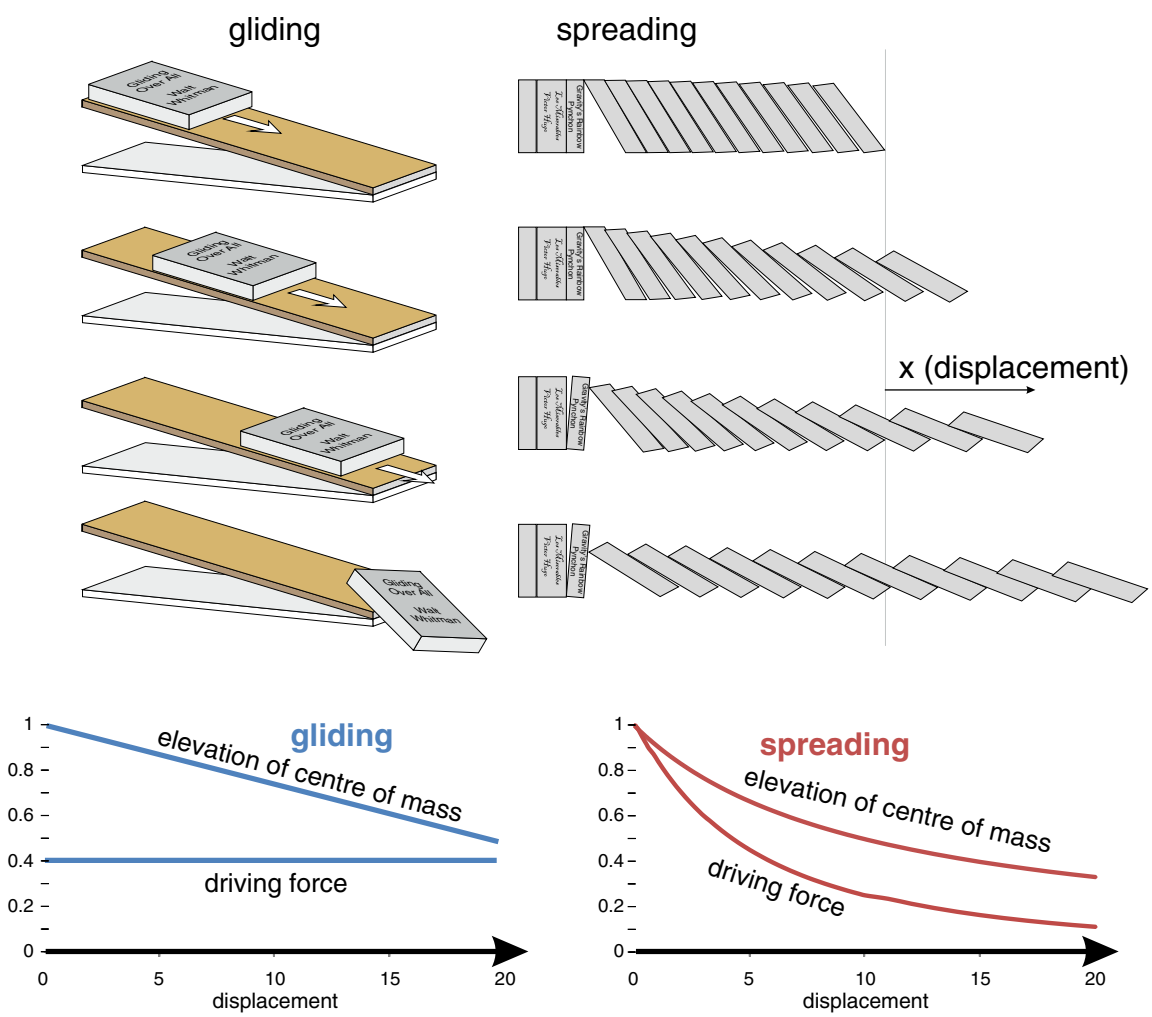

Fig. 5. Accidents in the library, illustrating the different behaviour of gliding vs. spreading. The gliding example (top left) is a book sliding down an inclined shelf. The spreading example (top right) is a set of books whose overall shape changes as the set deforms. The driving force is proportional to the loss of height of the centre of mass per unit distance travelled. Note that this may be constant for a gliding system (bottom left), but in contrast it diminishes with distance for a spreading system (bottom right), unless the system is refuelled by addition of more sediment.

and the most effective way to resupply is by deposition of new sediments on the updip part of the system. Without energy resupply by new sedimentation, energy considerations alone indicate that a spreading system has the most driving force at the beginning of translation, and as the driving force wanes it should slow down and eventually stop. This is dealt with in more detail in Section 6.1.

3.3. Quantifying the relative energy release in complex systems

In order to use the geometric analysis proposed here, we need to know the direction of movement of the centre of mass of the system as shown in Fig. 4. Because few natural examples are as simple as the schematic examples of Fig. 5, a systematic method was developed to provide an estimate of the magnitude and direction of movement of the centre of mass. This method can be applied to any complex system where we can define the displacement of every point (for example, in numerical forward models, or in experimental models with particle tracking) and in any real-world section for which there is a valid and reasonable palinspastic restoration (reconstruction to geometry at past times) which define the finite displacements for a large number of representative points. A simple graphical method is developed which provides an effective short cut for this process.

The full solution is to calculate the energy contributions from gliding and spreading of every unit cube, and then to sum these over the whole body. The approach, shown in Fig. 6, is essentially the same as that set out in Fig. 4. The displacement vector n is resolved first into the components of movement parallel to, and perpendicular to, the base. These are then resolved again to obtain the vertical movement resulting from motion parallel to the base, $\Delta z(\text{glide})$, and the vertical movement resulting from motion perpendicular to the base, $\Delta z(\text{spread})$. Multiplying these by the effective weight of the unit cube defines the energy contribution from gliding and spreading of the unit cube. The gravity gliding component of energy release due to motion of the unit cube $= W\Delta z(\text{glide}) = t^3(\rho(\text{sed}) - \rho(\text{fluid})) * g * \Delta z(\text{glide})$.

The gravity spreading component of energy release due to motion of the unit cube $= W\Delta z(\text{spread}) = t^3(\rho(\text{sed}) - \rho(\text{fluid})) * g * \Delta z(\text{spread})$, where W is the effective weight of the unit cube, accounting for buoyancy, g is the acceleration due to gravity, t is the dimension of the unit cube, $\rho(\text{sed})$ is the density of the sediment, and $\rho(\text{fluid})$ is the density of the overlying fluid[3]. Summing the energy contributions from every unit cube over the relevant area of the section (the region over which movement releases potential energy, as shown in Fig. 1) defines the total energy contribution of spreading vs. gliding per unit width of section.

The full solution method takes into consideration variations in sediment density across the system, but it is a cumbersome and complicated process. However, if the density is relatively uniform, or a less exact solution which assumes uniform density is sufficient, the analysis can be greatly simplified. In this case, we obtain the same solution if instead of calculating the energy contribution of each unit cube separately; we can instead calculate the average movement vector and apply this to the whole of the relevant area. The vector sum of the individual cell vectors is calculated (Fig. 7), then as before this is resolved into the base-parallel and base-perpendicular components, and the vertical component of these is calculated ($\Sigma\Delta z(\text{glide})$ and $\Sigma\Delta z(\text{spread})$, respectively). Finally the mean values $\overline{\Delta z}(\text{glide})$ and $\overline{\Delta z}(\text{spread})$ are calculated, representing the vertical movement of the average point due to gliding and spreading.

[3] For gravity failures in different settings, use appropriate densities for the overlying fluid: seawater, fresh water or air, as appropriate (other fluids may be used in planetary settings).

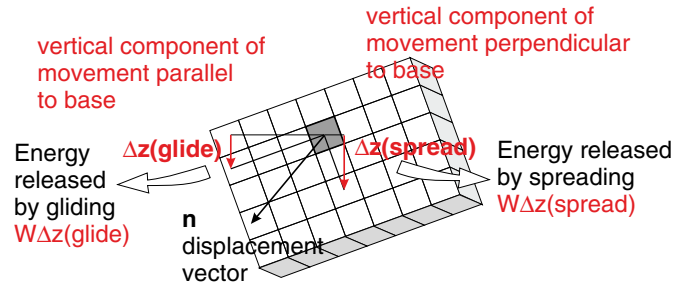

Fig. 6. Vector resolution of the finite displacement vector of a unit cube within the larger system, defining the energy contribution due to spreading and gliding. Key: n = displacement of the unit cube, Δz = change of elevation, W = effective weight of the unit cube.

From this we can calculate the energy contribution of the two components across the whole section:

$$\text{Energy release (per unit thickness along strike) of the whole section due to gliding} = W\overline{\Delta z}(\text{glide}) = Atg(\rho(\text{sed}) - \rho(\text{fluid}))\overline{\Delta z}(\text{glide})$$

$$\text{Energy release (per unit thickness along strike) due to spreading} = W\overline{\Delta z}(\text{spread}) = Atg(\rho(\text{sed}) - \rho(\text{fluid}))\overline{\Delta z}(\text{spread}).$$

If we are interested in the relative contribution made by gliding and spreading, rather than the absolute energy release, the analysis becomes simplified further still. A dimensionless number, α, expresses the proportion of total energy contributed by spreading, which defines where the system lies on the spreading/gliding spectrum.

$$\alpha = \text{Proportion of total energy contributed by spreading} = \overline{\Delta z}(\text{spread})/\overline{\Delta z}(\text{spread}) + \overline{\Delta z}(\text{glide}).$$

An α value of 1 corresponds to pure spreading, with no energy contribution from gliding. α value of 0 corresponds to pure gliding, with no energy contribution from spreading.

4. Quantification of gravity spreading and gravity gliding in synthetic, forward-modelled sections

4.1. A simple gliding/spreading nappe

FROGGGS (forward realisation of gravity gliding/gravity spreading) is a forward-modelling application written by the author to create and analyse simple systems of gravity-driven deformation. An initial 3-layer stratigraphy, which can be uniform or non-uniform, is deformed and translated using a user-defined deformation scheme. Nodes on the model are tracked, and a displacement vector field is calculated. In the example shown in Fig. 8, a uniform layered stratigraphy, tilted at 5°, deforms by uniform plane strain. This style is similar to the experimental gliding–spreading nappe model analysed by Brun and Merle (1985).

If the 60 cells of this model are scaled as 1 km × 1 km blocks, comprising an initial stratigraphy 3 km deep by 20 km long, with an average sediment density of 2100 kg/m^3 for the sediment, the potential energy released by the movement is 0.35 PJ/m (PetaJoules per metre of along-strike width of the model, where 1 PJ = 10^{15} J), consisting of 0.24 PJ/m contributed by spreading and 0.12 PJ/m from gliding. The spreading/gliding factor for this model, α, has the value 0.68, indicating a spreading-dominant system with some contribution from gliding.

4.2. Forward-modelled raft tectonics with varying basal dip angles

The FROGGGS application can model any user-defined deformation pattern. The geometry shown in Fig. 8 is a simple one to illustrate the

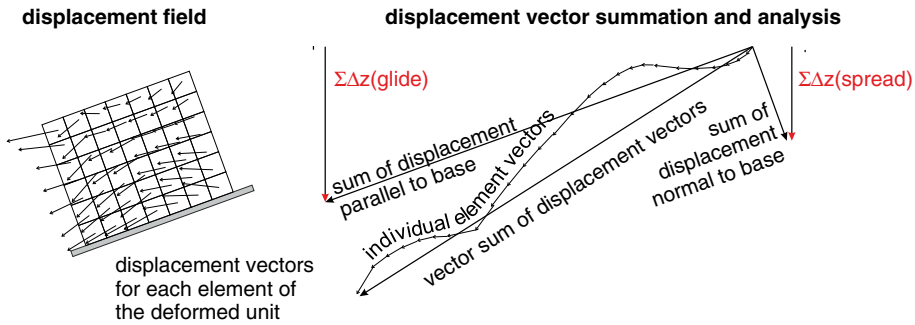

Fig. 7. Summing the displacement vectors to derive the net vertical displacement due to gliding and due to spreading.

process; this style of deformation resembles that of a pure salt body on a slope, but it is not a full characterisation of that scenario.

The advantage of this forward-modelling approach is that it allows the effect of changing one variable alone to be investigated. This is shown in a more geologically reasonable model, shown in Fig. 9. This model, designed to mimic the scale and style seen in some passive margin settings, consists of a series of raft blocks above a basal detachment. The model consists of 180 nodes, and it corresponds to a system 60 km long by 3 km thick.

The effect on the energy budget of changing the dip angle of the basal decollement was investigated, for dips ranging from 20° downwards to 4° upwards in the movement direction. The results, shown in Fig. 9, show that for basal dips less than 8°, the energy budget of this geometry is spreading-dominant, and above 8° its energy budget is gliding dominant. This result is quite surprising: most geologists would intuitively describe this geometry as being characteristic of gravity gliding. However, the decollement dips seen on real-world continental margins are typically in the range of 0–5°, and within that range the model results fall squarely into the spreading-dominant category. In the top example, the basal decollement dips upwards in the direction of transport, so that the gliding component results in net absorption of energy.

An important conclusion of this exercise is that the angle of dip of the basal decollement is not, by itself, sufficient to diagnose gliding-dominant vs. spreading-dominant systems: if the base is horizontal or upwards-dipping we can be sure that spreading is the dominant component, but if the base dips in the transport direction, we need to carry out an energy calculation to determine which component is dominant.

Cross plotting the relative contribution of gliding vs. spreading, as shown in Fig. 10, emphasizes the point that for this geometry it is impossible to achieve an α value of 0, corresponding to pure gliding, and that for most geologically reasonable dips this model is spreading-dominated.

5. Quantification of gravity spreading and gravity gliding in natural examples

5.1. Defining displacement vectors

This approach can be applied to real-world systems using a present-day depth section (e.g. Fig. 11a) and a valid palinspastic restoration, or suite of restorations to different times in the past (e.g. Fig. 11b). The depth section may be created from any appropriate data source (seismic reflection data, well data, outcrop information, etc.). Points that can be identified on both the present day and restored sections are used to define the displacement vector (Fig. 11c).

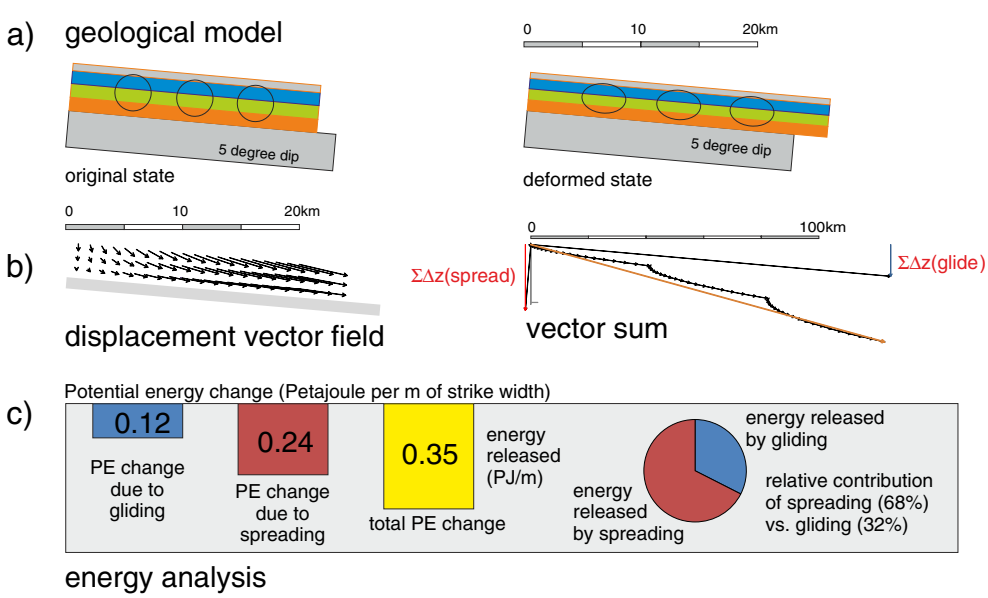

Fig. 8. FROGGGS forward-modelling and analysis of a deforming sediment sequence, in which the base dips at 5° downwards in the movement direction. a, geological model for the deformation, showing the pre-deformation and post-deformation geometries. b, vector analysis, showing the displacement vector field (left) and the vector summation (right). The cusps on the vector summation plot result from the order in which data points are sampled, which takes the data from each layer in turn from left to right. c, energy analysis showing the absolute and relative amounts of energy released by gliding and by spreading.

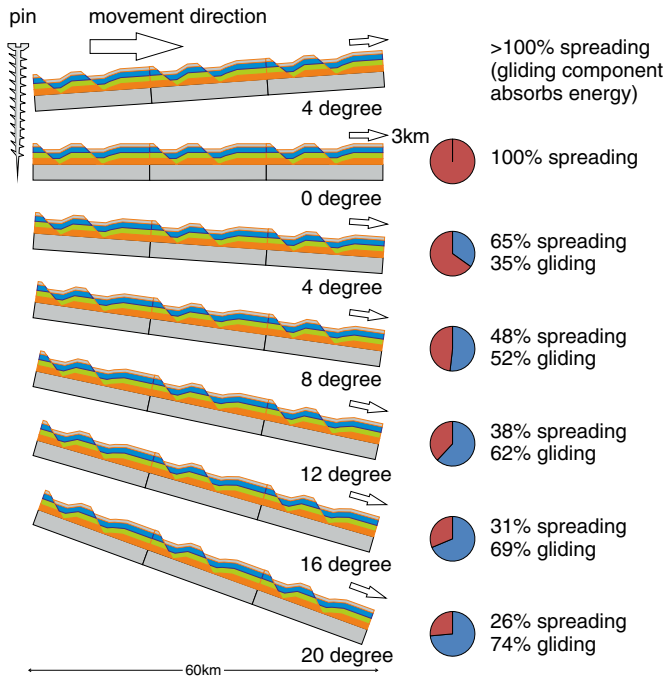

Fig. 9. FROGGGS forward-modelling and analysis of a 60 km × 3 km thin-skinned gravity failure consisting of raft blocks and listric faults, in which the basal decollement dip is varied. The displacement field is the same for each model, with transport towards the right. The pie charts show the relative contribution of spreading vs. gliding calculated in the same manner as shown in Fig. 8. In all cases shown here, energy is released by the spreading component of movement. In the top section, the basal decollement dips upwards in the direction of transport, so that energy is absorbed by the movement parallel to the base (the gliding component), but this is outweighed by the energy released by spreading.

The simplest type of point to match is the intersection of a stratigraphic horizon with a fault. If the restoration is to a continuous unfaulted bed, as shown in Fig. 11b, then a single point X on the restored section matches two points (X′ and X″) on the deformed section.

The displacement vectors can also be determined for synkinematic sediments; for these the vector links the point where the particle was deposited with its current location, and for this a sequential restoration series may be required.

The method described above in can be used to define the movement vectors by comparison of the present day and restored sections, or in principle between two palinspastic sections representing the geometry at different times. The displacement vectors represent the net movement between the time represented by the two sections, and the energy calculations will represent the net behaviour of the system between those times. The restored section to which the comparison is made does not have to be to a fully prekinematic state. However, if we are interested in measuring the total energy contributions of gliding vs. spreading

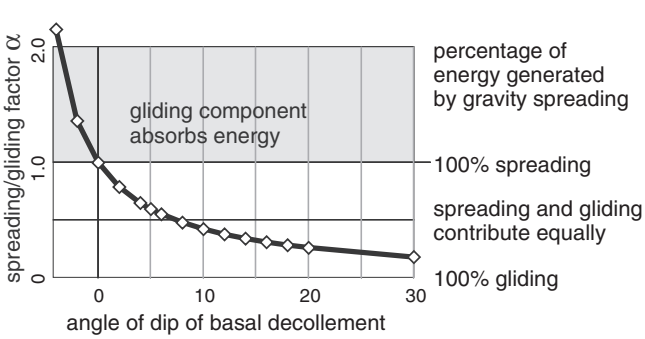

Fig. 10. Energy budget analysis for the model shown in Fig. 9 shows how the relative contribution of gliding vs. spreading varies with dip, based on the analysis of 15 models.

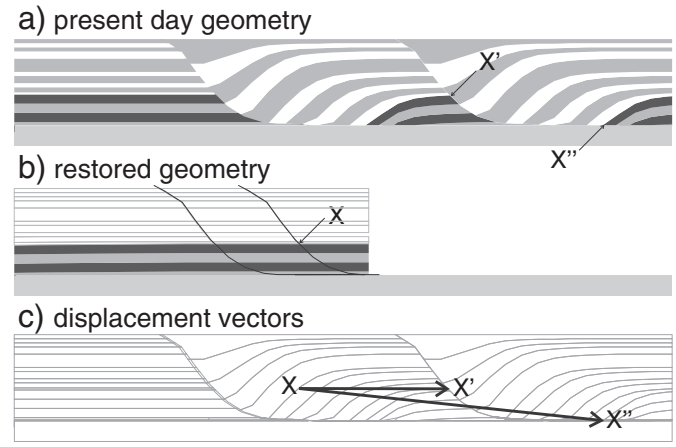

Fig. 11. Identification of common points on the present day section (a) and restored section (b) defines the net movement vector (c). Synthetic cross section was created by the author.

over the lifetime of the system, the initial restored section should be to a pre-kinematic geometry. The contribution of synkinematic sediments is defined by identifying the position of a point in those sediments at the present day and its position at the time that it was deposited. To do this may require analysis of a suite of sequential restorations.

5.2. A natural example from the Orange Basin margin, South Africa

The Orange Basin example of Fig. 1 was analysed in this way (Fig. 12). The gravity tectonic system is a good candidate for the method because the whole of the system is moderately well imaged on seismic data (de Vera et al., 2010) and the restorations are well-constrained (the horizons can be correlated with confidence, and there is no complicating factor such as salt). Points identified on the present-day depth section (Fig. 12a) and a set of palinspastic restorations created by the author (Fig. 12b–d) were used to define the movement vectors (Fig. 12e), of which 52 vectors lie within the main extensional region. The vectors were summed (Fig. 12f) to derive the average displacement of a particle within the body of the extensional system (a displacement of 8.0 km with a dip angle of 3.1°). This was resolved in the usual way into components parallel to and normal to the base of the system (which dips at 2.06°), and then finding the vertical component of these.

The vertical descent of the average particle is 433 m, which breaks down as 145 m descent due to gravity spreading and 288 m due to gravity gliding. Assuming a mean sediment density of 2100 kg m^{-3} this gives an energy contribution of 80 TJ/m of strike width due to spreading and 160 TJ/m due to gliding.

The spreading/gliding factor for this model, α, has the value 0.32, and so this is a gliding-dominated system with a lesser contribution from spreading.

5.3. Application to the Lower Kwanza Basin, Angola

Application of the method to a margin involving detachment on salt was tested on a section from the Lower Kwanza Basin of Angola, modified from Peel et al. (1998), shown in Fig. 13. This was chosen because of the availability of high-definition versions of the present day and restored sections.

The Angola Kwanza margin is dominated by thin-skinned detachment of the Late Aptian to Recent section on Aptian salt. Large-scale basinward movement has separated the carbonate sequence which lies immediately above the salt into raft blocks separated by younger siliciclastic sediments (Burollet, 1975; Duval et al., 1992; Lundin, 1992; Mauduit et al., 1997). The base-salt surface dips overall towards WSW, but this dip is far from uniform: the base-salt surface is offset

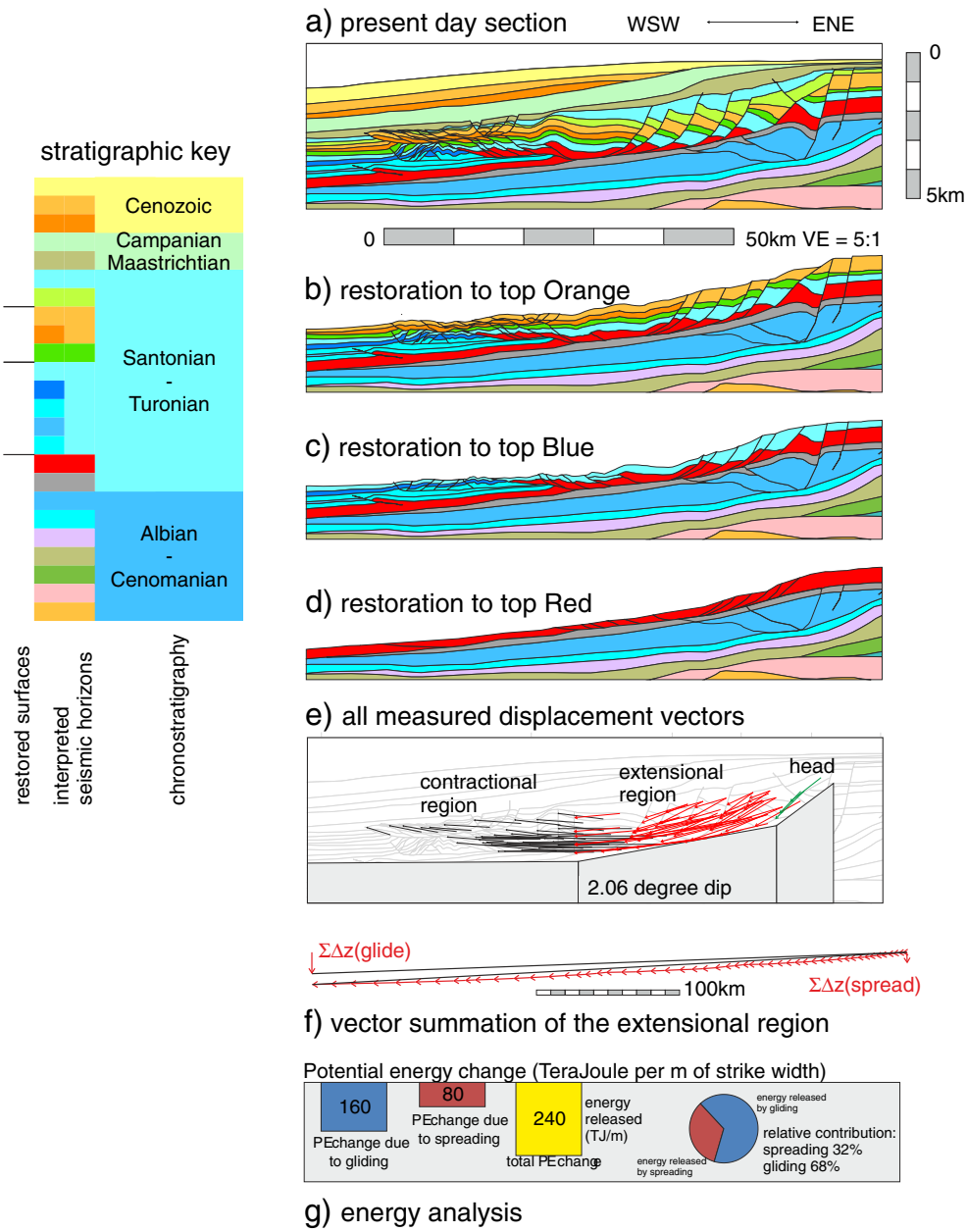

Fig. 12. a, balanced cross section from the Lower Orange Basin of offshore South Africa interpreted and restored by the author. b–d: palinspastic restorations. The present-day section, the restorations and the measured displacement vectors (e) are all shown with 5:1 vertical exaggeration; the vector summation and resolution (f) is shown with no vertical exaggeration. The restorations were made by the author using block movement, rotation and vertical simple shear. No decompaction is applied. The energy analysis (g) shows that this is a gliding-dominated system (68%) with some contribution from spreading (32%).

by a steep region, the Atlantic Hinge Zone with an average dip of 4°, separating regions of much lower dips (0.7°) to the east, here labelled the shelf/upper slope zone, and to the west (1.25°), here labelled the lower slope zone (Hudec and Jackson, 2002, 2004; Jackson and Hudec, 2005; Marton et al. 1998; Peel et al., 1998; Rowan et al., 2004).

As the cover sequence moves over the steep zone, a ramp syncline basin (Benedicto et al., 1999; Ellis and McClay, 1988) is formed and progressively filled with sediments. The distinctive stratal architecture of this basin indicates where each sequence lay relative to the ramp edge at the time of deposition, allowing a relatively precise sequential restoration to be made (Hudec and Jackson, 2004; Jackson and Hudec, 2005; Marton et al., 1998; Peel et al., 1998; Rowan et al., 2004). The upward transition from carbonate-dominated sediment to a sequence dominated by clastic sediment and marl is a distinctive and unequivocally correlatable seismic horizon, marking the boundary between what is labelled here the "post-salt-1" interval (mostly carbonate) and the overlying "post-salt-2" interval. A restoration to this surface (Fig. 13c) is used as the reference from which displacements were measured (Fig. 13d). The initial section and the palinspastic restorations were constructed using LOCACE® software (Moretti et al., 1990).

The structural style of the Atlantic Hinge Zone and the area updip of it are dominated by extension and lateral translation: the region downdip of the Atlantic Hinge Zone is dominated by contraction (here by folding) and salt diapirism.

Every point that could be identified on both the present and restored section was identified and used to construct a set of displacement vectors (Fig. 13c). These were grouped into sets which lie entirely in the lower slope zone (12 measurements), those which include movement across the Atlantic Hinge Zone (17 measurements) and those which lie entirely within the shelf/upper slope zone (35 measurements).

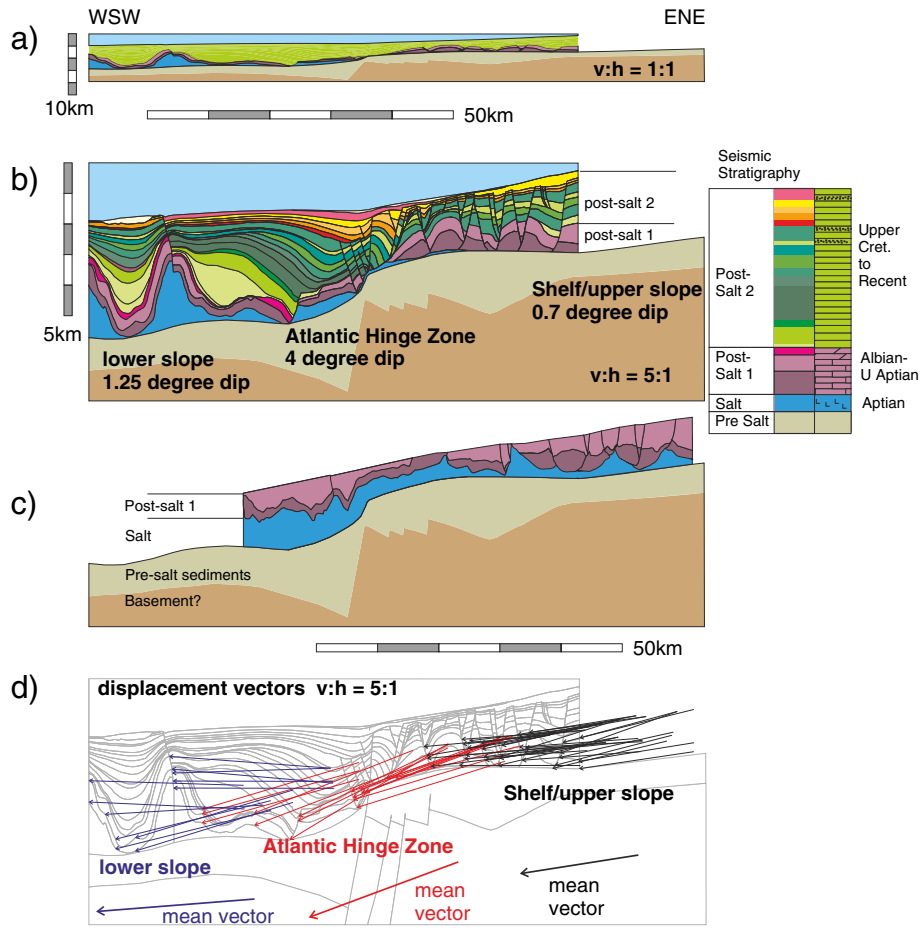

Fig. 13. Restored cross section from the Lower Kwanza Basin, based on depth-converted seismic reflection data, from Peel et al. (1998). Interpretation and section construction/reconstruction are by the author. a) Present-day depth section with no vertical exaggeration, in which the post-salt stratigraphy is divided into two intervals; b) present day section with 5:1 vertical exaggeration, showing all interpreted seismic horizons; c) restored cross section to geometry at the end of deposition of "post-salt 1" interval; d) measured displacement vectors.

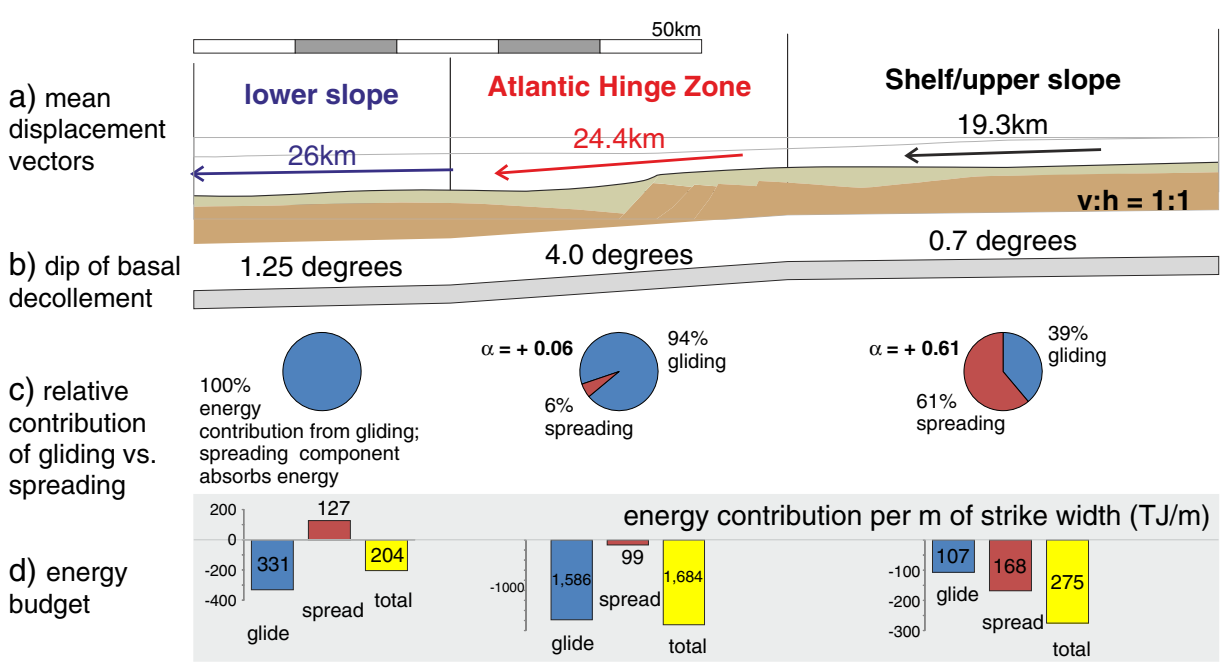

Fig. 14. Vector analysis and energy contribution of the gliding and spreading mechanisms to the segments of the section shown in Fig. 13. The vectors and the depth section (a) are shown with no vertical exaggeration. The bar chart (d) shows the estimated absolute energy contribution, per metre of strike width, for the different components in TeraJoules per metre of strike width.

These data were then used to derive the average movement vector for each of the three zones, and then from this the relative contribution of gliding and spreading to the energy budget was estimated in the method described previously. The results, shown in Fig. 14, show a striking difference between the three regions.

Energy contribution to the shelf/upper slope region is dominated by spreading (61%) with a lesser contribution from gliding (39%). In contrast, the Atlantic Hinge Zone region is dominated by the contribution of gliding (94%). The lower slope region is interesting because the two components act in contrary direction. In this region, the mean basal slope dips very gently westwards (1.25°) so that westward movement releases potential energy; therefore in this region gravity gliding is a net positive contributor. However, deformation in this region is contractional, so that instead of lowering the centre of mass and thereby releasing energy (normal spreading), the deformation raises the centre of mass and absorbs energy. The positive contribution of gliding outweighs the energy absorption from deformation, so this region is still a net contributor to the gross energy budget.

Using the same assumption for bulk sediment density as before, we can estimate the absolute energy contributions (Fig. 14d) which reveal that the energy released in the relatively narrow Atlantic Hinge Zone is greater than the entire rest of the section.

The main lessons to be drawn from this exercise are that:

(i) The method appears to be robust and consistent, and can be applied with ease to a section for which a valid suite of restorations exist.
(ii) The shelf/upper slope region of the Kwanza margin is dominated by gravity spreading on this section.
(iii) The steep zone around the Atlantic Hinge Zone is dominated by gravity gliding on this section.
(iv) There are considerable differences in behaviour between different parts of the same line, arising from the great difference in basal slope angle, and it would be inappropriate to characterize the whole line based on an average dip and an average behaviour.

These lessons run contrary to the statement "the Angolan margin is thought by many to be a gravity-gliding system" (Schultz-Ela, 2001, referencing Mauduit et al., 1997). In order to investigate whether this is a local anomaly, a second line was analysed from a different region of the same margin.

5.4. Application to the Lower Congo Basin margin, Angola

The Kwanza example described above was facilitated by access to high-resolution graphics of the present-day and restored sections. To further test the method it was applied to a cross section from the Lower Congo Basin of Angola, using only published images.

Marton et al. (2000) presented a section (their transect B) through the Lower Congo Basin of Angola, showing its present day geometry, and a suite of palinspastic reconstructions, of which one is shown in Fig. 15. On this transect, there is no steep region equivalent to that seen in Fig. 13. The basal decollement has a fairly uniform dip of around 1.3° and therefore there is no need to analyse subareas of the section in the manner described for Fig. 13.

Bitmap images of the sections from Marton et al. (2000) were scanned. The graphical approach described above was used to estimate the relative contribution of gliding and spreading to the energy budget for this section. The vector analysis was carried out only for the energy-releasing region, corresponding to the regions of extension and translation, but not including the contractional region. This focus is required because the diagnosis of gliding vs. spreading is obtained from the region of net potential energy release.

The cross section was scanned and stretched to remove vertical exaggeration. The restoration was modified slightly, reducing the thickness of the salt layer in order to correct a problem (salt volume imbalance) present in the original work. 46 points that could be easily matched on both the present day and restored section were identified, and vectors drawn showing the net displacement for each of these points (Fig. 16a). These vectors were summed as before (Fig. 16b) and the average vector calculated. For these points, the average displacement was 4.2 km, dipping at an angle of 5.2° from horizontal (Fig. 16c). For comparison, the average dip of the basal decollement is 1.3°. Resolving this into components as before to obtain the spreading/gliding factor for this model, α, gives the value 0.75, indicating a spreading-dominated system with a small contribution from gliding.

This is again contrary to the perception, referenced by Schultz-Ela (2001), that the Angola margin is a classic example of gravity gliding. Two reasons may explain why prior perception of the Angolan margin

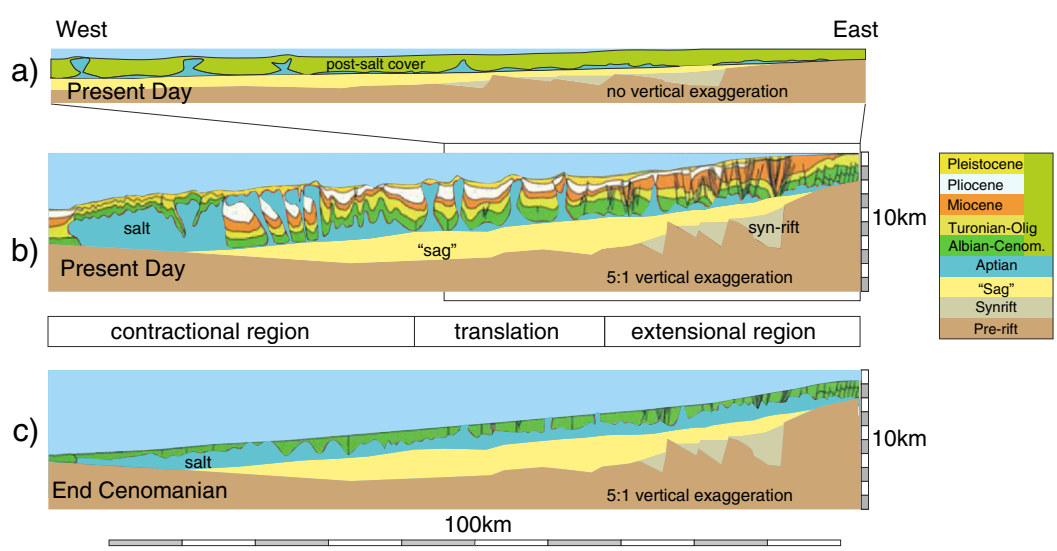

Fig. 15. Cross section through the Lower Congo Basin and restoration to end-Cenomanian time. a) Updip part of the present day section with no vertical exaggeration, showing true dips; all post-salt sediments have been grouped together for clarity; b) present-day section, at 5:1 vertical exaggeration, unmodified from the original other than recoloring the salt; c) section restored to end-Cenomanian time. The restored section has been slightly modified to minimize salt volume imbalance: the thickness of the salt has been reduced relative to the original, but the geometry of the suprasalt sediments is unchanged. See original publication for key to stratigraphy.
Redrafted from Marton et al. (2000).

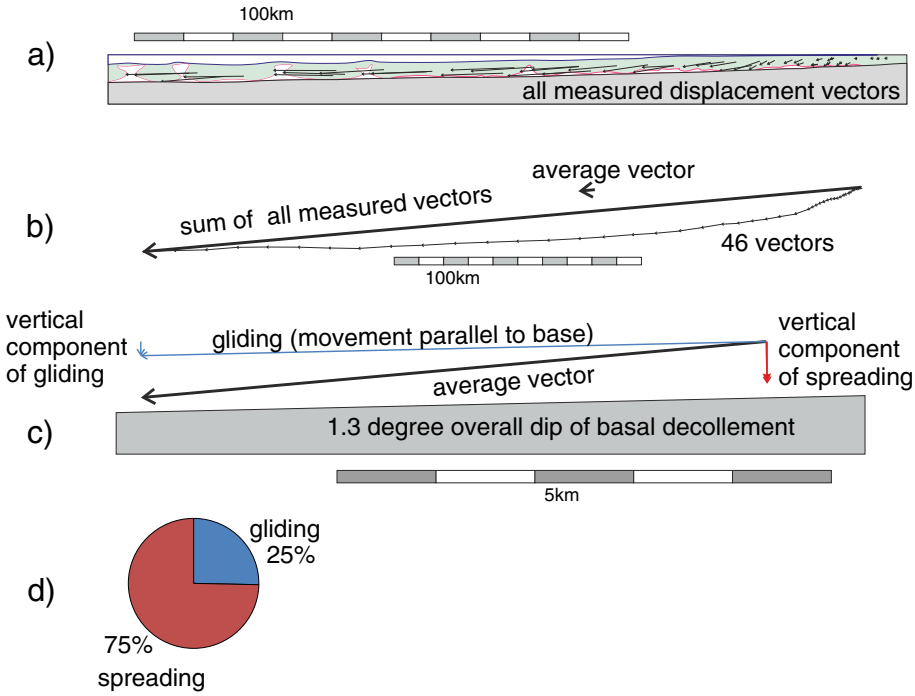

Fig. 16. Gliding/spreading analysis of Marton et al. (2000) section carried out using graphic method; a) measured displacement vectors, superimposed on an outline of the extensional and translational part of the present day section with no vertical exaggeration; b) vector summation and construction of the average displacement vector; c) resolution of the average displacement into its gliding and spreading components (parallel to and perpendicular to the basal decollement; d) the relative energy contribution from gliding (25%) and spreading (75%).

differs from the results of this quantitative analysis. Firstly, prior to this contribution there has been no method for directly measuring the relative contribution; secondly, sections are commonly displayed with vertical exaggeration (Stewart, 2011) which gives a misleading impression of steepness. The actual average dip on this transect is only 1.3°, illustrated to scale on Fig. 16c. Since this is so close to horizontal, even a large displacement parallel to the base generates very little energy; systems with very basal dip angles therefore tend to be dominated by gravity spreading, as demonstrated by the FROGGGS modelling (Fig. 9).

We may apply this insight by inspection to other lines through the same margin. A regional line through the Kwanza margin, from Rowan et al. (2004) (Fig. 17), clearly consists of three zones: a shelf/upper slope region in which the basal decollement has very low dip, a steep zone, and an outboard region of low dip. Visual comparison with the detailed analyses described above (Figs. 13–16) suggests that this section probably divides as shown into regions dominated by spreading, by gliding, and a region of contraction (negative spreading).

6. Discussion

6.1. Relationship of deformation to sedimentation

An important difference between spreading-dominant systems and gliding-dominant systems is that for gravity gliding, the driving force of may not diminish with distance travelled (Fig. 5c), whereas in a spreading system, the driving force of necessity diminishes with distance travelled, given a uniform basal slope, and in the absence of ongoing sedimentation.

This is clearly shown the analysis of a block of sediment deforming by pure gravity spreading, initially 10 × 10 × 2 km in size (Fig. 18). The elevation of the centre of mass drops with the inverse of the displacement; the driving force (energy released per unit distance) drops more rapidly, and the rate of movement (calculated assuming that the speed is proportional to the force per unit plan view area) more rapidly still. The same values plotted against elapsed time (Fig. 18c) show an even more precipitous decline. Applying this decline curve to a gravity-spreading system fuelled by pulses of sedimentation (Fig. 18d) shows that movement a spreading-dominated system may be very strongly linked to deposition, and therefore may be expressed as phases of deformation. In contrast, an idealized gliding system may move more or less independently of deposition.[4]

From this simple analysis, it is clear that in a spreading-dominant system, movement that is long-lived and which occurs at a sustained rate can only happen if the engine of the system is refuelled (i.e. the gravitational potential energy supply is renewed). This may result from progressive tilting of the margin (due to thermal subsidence, isostatic loading, etc.) or from updip sedimentation.

Thus we expect to see a strong temporal relationship between major depositional episodes and major phases of gravity-driven movement for a spreading-dominant system, as shown schematically in Fig. 19. In contrast, a gravity-gliding dominant system, such as the section moving over the Atlantic Hinge Zone in the Lower Kwanza of Angola, is likely to continue moving more or less continuously, independent of the depositional history.

6.2. Topography of the shelf and slope

The predicted difference in behaviour (dependence of major phases of movement on major phases of updip deposition in a spreading system, and relative independence in a gliding system) has important implications for the development of sea floor topography.

If deposition and movement are strongly coupled, as predicted for a spreading system, we expect that the main episodes of creation of accommodation space by movement should correspond to the major phases of sediment input, and in consequence the structurally-generated accommodation space is likely to be largely filled with

[4] This analysis is purely geometrical and does not take in to consideration other aspects of the response of the sediment unit to deposition. For example, rapid sedimentation may induce elevated pore fluid pressures throughout the sediment body, resulting in weakening and failure (Masson et al., 2006).

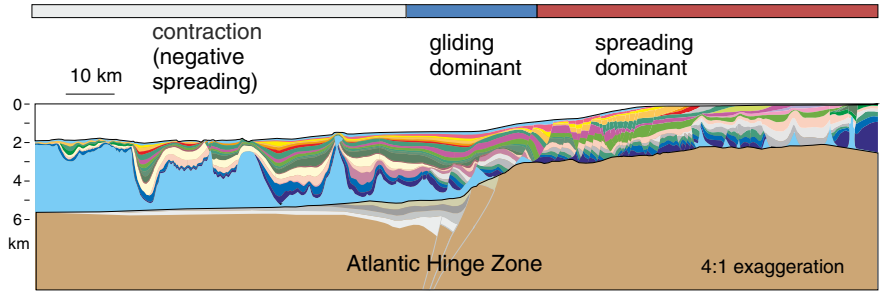

Fig. 17. Regional section through the Lower Kwanza Basin, Angola. Vertical exaggeration 4:1. From Rowan et al. (2004).

sediment (as shown in Fig. 20a). This results in relatively suppressed bathymetric relief and a potentially weak degree of structural control on bathymetry. During sustained periods of low overall sediment input, the model predicts that movement of a spreading-dominated system will slow down or stop, so that the creation of accommodation space is inhibited: as a result deep relative topography related to lateral movement is unlikely to develop.

In a gliding-dominant system, major phases of movement are not hard-linked to major phases of sediment input. During periods of major sediment input, the bathymetric response will be similar to that of a spreading-dominant system (Fig. 20a), but during periods of low sediment input, continuing structural movement may open up holes faster than they are filled with sediment, resulting in a different stratal architecture, and the possibility of deep-water troughs opening up in the shelf and upper slope (Fig. 20b).

6.3. Way forward

6.3.1. Future application of the analytical method to other examples

The analyses presented in this paper demonstrate that the method appears to be simple and robust. Although it has so far been limited to a few examples, its success in application to margins of different type, with different dips, different dominant mechanisms, and to salt floored and salt-free examples, indicates that it is generally applicable.

The method can in principle be applied to any cross section through a gravity-driven system for which a valid restoration or suite of restorations is available. Because construction of such sections is a common staple of regional structural analysis, many suitable sections exist in university and company archives, which can be readily analysed, and which could provide a large number of analytical results characterising margins around the world on the spectrum of gravity spreading vs.

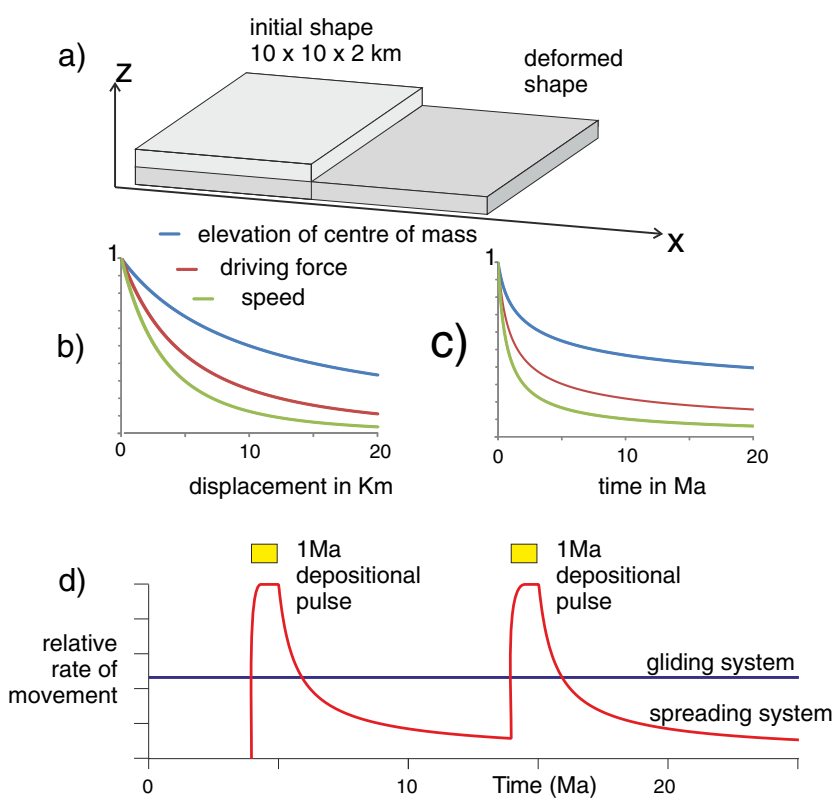

Fig. 18. a: sediment mass deforming by pure gravity spreading, initially 10 × 10 × 2 km. b: elevation of the centre of mass in km, the driving force (energy change per unit distance of displacement), and the speed of the front of the block, plotted against the distance travelled. c: the same values, plotted against elapsed time. Driving force and speed are normalized to an initial value of 1. Speed is calculated using parameters (density, viscosity of decollement layer) chosen to give an initial rate of 5 km/Ma for the front of the block, and assuming that speed is controlled by driving force per unit plan view area. d: the response of gravity-driven systems to a major depositional pulse. A pure spreading system (with the same parameters as b and c) gives a pulsed response (sawtooth curve); for an idealized pure gliding system the movement rate is steady.

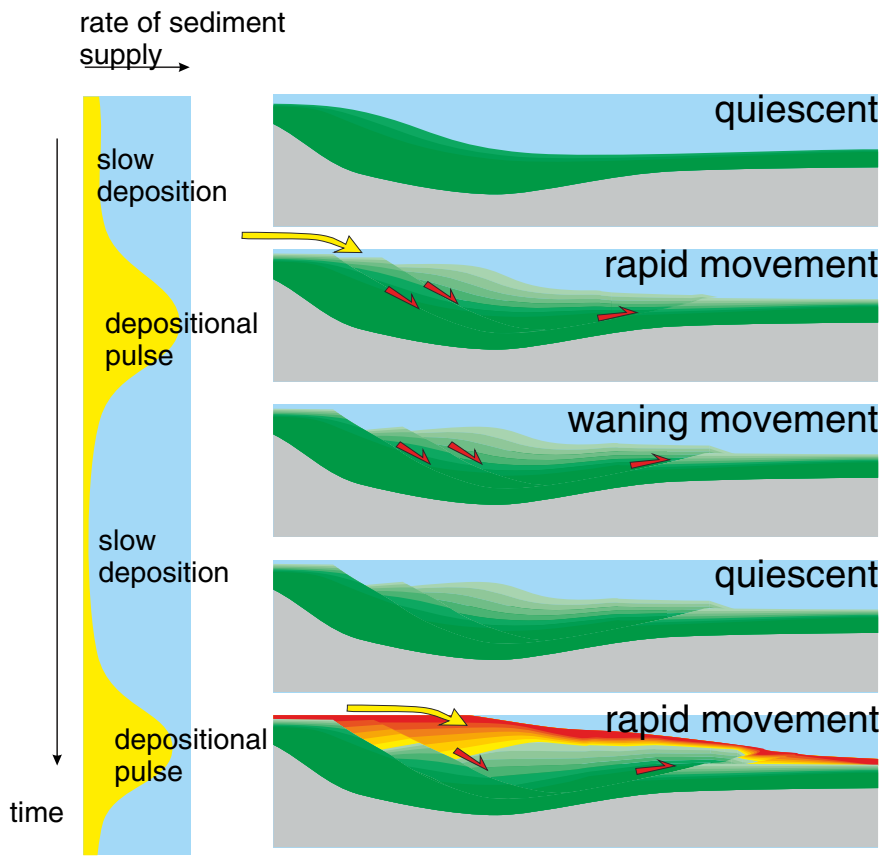

Fig. 19. Phased movement of a schematic gravity spreading system, related to major phases of sediment input.

gravity gliding. The author welcomes the opportunity to collaborate with other structural geologists to create an open data set of such analyses.

6.3.2. Recognition of the products and consequences of spreading vs. gliding

It would be useful to compile a list of features and observations that correlate with the dominant process, which might be used as evidence where a full energy analysis is not available. Recognition of particular behaviours, processes or features which are associated with spreading or sliding will also shed light on the geological processes at work.

6.3.3. Automation

The natural examples shown in this paper were analysed manually; particle paths were identified only for points which were clearly identifiable in both the present day and restored sections, such as horizon/fault intersections. However, computer-based structural restoration software should be capable of defining displacement vectors for any point within the restored section, allowing automated production of a greater number of reliable displacement vectors. It is reasonable to expect that these could be analysed automatically to create a more thorough and reliable analysis. If material properties of the sedimentary sequence, including its density structure, are defined for each point, it

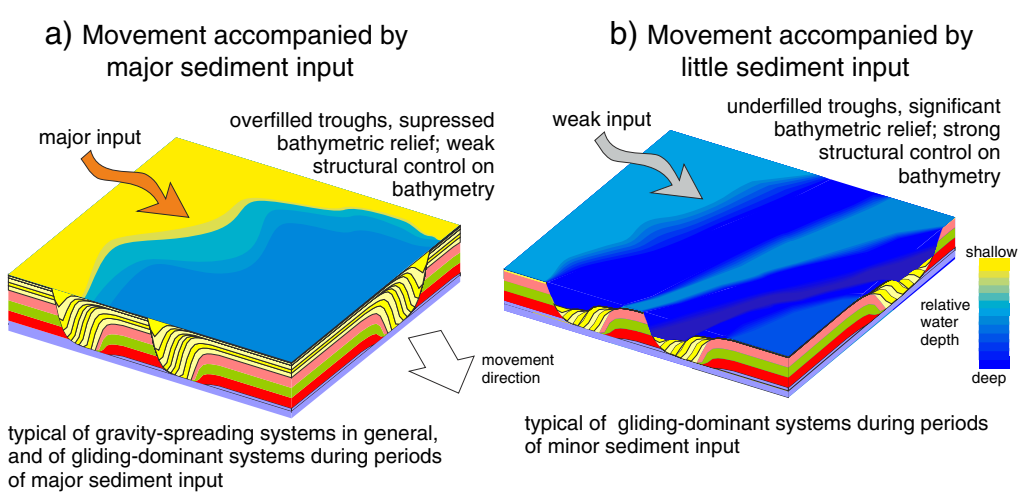

Fig. 20. Relative development of topography in a region of active thin-skinned extension, in which the region is (a) abundantly sediment-supplied, or (b) sediment-starved. Vertical exaggeration 4:1.

should also be possible to create a full energy analysis without making the simplifying assumption of uniform density.

6.3.4. From driving mechanisms to the energy balance of the whole system

This study has been focussed on the updip, energy-releasing part of the systems, because the driving mechanism is defined by this region. A similar approach can be applied to the whole of the system, including the downdip portion where movement stores gravitational potential energy, rather than releasing it. The centre of mass may be raised by pushing the sediments bodily up a dipping ramp, or by deformation which results in shortening and thickening of the sediment mass. These processes are the mirror image of gliding vs. spreading. As shown in Fig. 12e, displacement vectors may be measured in this region, and a parallel analytical method can be applied there. Quantifying the total potential energy of the whole system, including both the release and the storage of gravitational potential energy, is a necessary first step towards analysing the full energy balance of gravity-driven systems. The full energy balance of gravity driven systems will be explored in companion research. Understanding the energetics of gravity-driven systems as a whole will contribute towards our understanding and exploitation of them.

7. Conclusions

Returning to the original definitions of gravity gliding and gravity spreading of Ramberg (1967, 1977, 1981a,b) allows these to be clearly distinguished. The critical difference is the mechanism by which gravity supplies energy into the system: lowering the centre of mass by movement towards the base of the system (spreading), which requires internal deformation, or by movement parallel to the base of the system (gliding), which does not require internal deformation. Most natural examples are a combination of the two processes.

A simple geometric method allows the relative contributions of gliding and spreading to be quantified. This can be applied to a large body which has experienced complex heterogeneous deformation, by analysing a large number of small elements and summing the results.

Applying a uniform sediment density to the whole body allows further simplification. A single vector represents average movement of the whole entity, from which the spreading/gliding factor, α, can be calculated.

Forward-modelling of synthetic sections allows us to rapidly analyse geometries representative of natural gravity-driven systems, and to investigate the effect of changing single variables, such as the basal slope angle. This demonstrates that pure spreading or gliding is only achieved under exceptional circumstances. Most natural systems contain a mix of the two components, and real-world geometries are better represented by measuring the spreading/gliding factor, α, which shows where the system falls on the spreading/gliding spectrum.

Rigorous quantitative analysis of two regional lines from the margin of Angola demonstrates that large regions of this margin are dominated by gravity spreading, which contrasts with established wisdom based on qualitative methods.

Distinguishing the relative contribution of spreading vs. gliding is an important contribution to the understanding of passive margin deformation. Spreading systems deplete their energy supply (gravitational potential energy) in a way that is non-linear with respect to distance moved: hence the driving force diminishes unless the system is refuelled, most commonly by updip deposition. In consequence, there is a strong linkage between sediment supply and the movement of large-scale gravity spreading systems. In contrast, movement of gliding-dominant systems may be independent of sediment supply rates.

This has important consequences for the development of topographic relief above the gravity-driven system, and for the gross stratal architecture of synkinematic sediments within it. A systematic and quantitative study of these systems, using modern seismic data, is likely to have applications to hydrocarbon exploration and to studies of subsurface fluid flow processes in general.

Acknowledgements

The author gratefully acknowledges support by the UK Natural Environment Research Council (NERC) and the helpful reviews by colleagues at NOCS.

Appendix A. Constraints on the geometric method for distinguishing the contribution of spreading vs. gliding

A.1. Validity and format of the present-day section and palinspastic restoration

The geometric method proposed above assumes that the present day section is structurally appropriate and its restoration is both valid and reasonable. The sections must be in depth, not two-way time; they must be complete at least down to the basal decollement of the system. The vector analysis should be carried out on sections without vertical exaggeration.

The section should ideally include the whole updip portion of the linked system, including a point beyond the limit of extension which can be taken as fixed. This enables the true lateral displacement to be estimated through the process of palinspastic restoration.

In some circumstances, it is possible to determine the true lateral displacement by other means. This is the case in the Kwanza basin of Angola, where movement over the Atlantic Flexure creates a diagnostic record of displacement in the stratal patterns of the transported material (Hudec and Jackson, 2004; Peel et al., 1998; Rowan et al., 2004). In such settings, the method can be used effectively without requiring the section to be complete to the updip limit of extension.

For sections with a basal salt decollement, it is vitally important to create a palinspastic restoration in which salt has neither been gained nor lost, otherwise a systematic error is introduced. This can be mitigated by ensuring the palinspastic restoration is optimised and that salt volumes are balanced.

A.2. Reference frame, vertical movement

The reference frame used to compare positions in the present day and restored sections should be a point on the basal decollement surface. It is normal for the whole margin, including the transported material and its basement, to experience subsidence or uplift for a variety of reasons. This superimposed vertical movement must be removed from the calculation; choosing a point on the basal decollement in each section and measuring position relative to this point should achieve this.

A.3. Reference frame, tilting

The method assumes that the whole system, including the section below the decollement, has not tilted significantly during movement. In circumstances where there has been regional tilting, the method can still be used, but it will provide a range rather than a single value. The process to use in such cases is to rotate and move the whole restored section so that the sub-decollement section matches present-day in both dip and elevation. The displacement vectors are measured in the usual way. Then the spreading/gliding factor, α, can be calculated with the present dip (as though all the tilting occurred at the start of the process), for the original dip (as though all the tilting occurred at the end of the process) and for a mid-way dip. The range of α value represents the uncertainty.

Appendix B. Limitations on the method

B.1. Sampling bias due to incomplete stratigraphy in the restored section

If a suite of palinspastic restorations is available for multiple different times, points in the present-day section can be matched to previous positions for most of the section. However, if only one restoration is available, it is not possible to obtain displacement vectors for the upper layers of the stratigraphy which are absent in the restoration. This may lead to a systematic error, especially if a substantial synkinematic section present in large growth-faulted basins is not taken into consideration: omitting this section will tend to underestimate the relative contribution of spreading relative to gliding. This error can be mitigated by considering more sequential stages of restoration.

B.2. Bias due to the effect of sediment compaction

Vertical movement of the sediment sequence occurs due to compaction, in response to burial by younger sediment. This vertical movement does not contribute towards the energy budget of spreading or gliding. However, in the method set out here, it will appear in the calculation as an apparent contribution towards spreading. The effect of compaction will tend to overestimate the relative contribution of spreading, to some extent countering the sampling bias effect described above. On way to mitigate this compaction effect is to make the calculation based primarily on vectors derived for the deeper part of the stratigraphy, where the rate of compaction is less. There is no simple way to remove this effect entirely.

B.3. The effect of diapirism

Diapirism results in the upward movement of less dense material and the downward movement of more dense material. This movement is independent of, and does not contribute towards, the energy supply for gravity spreading or gliding. As long as a sufficient number of points are used to define the displacement vectors, and there is no sampling bias that oversamples either the uplifting or downgoing regions influenced by diapirism, the effect of diapirism should be removed by the averaging process. A good example of this is the downdip region of the Lower Kwanza section (Fig. 13d) which includes both the uplifted regions and the down dropped region between them.

Appendix C. Mechanism of palinspastic reconstructions used in this article

The vector analysis is dependent on the method of restoration or forward modelling and thus a brief discussion of this is justified.

Figs. 8–10: The FROGGGS forward models have a user-defined deformation. This can include pure shear and simple shear with axes parallel to the basal decollement. Deformation of the hanging wall of the minor faults in the FROGGGS models is accommodated by simple shear perpendicular to the basal decollement.

Figs. 13 and 17: the Lower Kwanza basin lines were interpreted, created and restored by the author. The present-day model is based on 2D seismic reflection data, interpreted and depth converted by the author. They were constructed and restored using LOCACE software (Moretti et al., 1990). Palinspastic restoration was carried out for each block in turn, in the following stages: (i) rigid translation (block movement and rotation), to take out fault displacement; (ii) deformation of the fault block to restore the top (depositional) surface to a reasonable geometry, based on a full stratigraphic-depositional model; (iii) deformation of the underlying blocks to remove any fault gaps or overlaps; (iv) decompaction of the collaged suprasalt blocks using LOCACE standard compaction curves. In the extensional domain, the primary deformation mechanism used was inclined simple shear. In the contractional domain, the primary deformation mechanism used was flexural slip.

The gap created between the collage of restored suprasalt fault blocks and the basement was assumed to be filled with salt. The salt area in each time step was calculated. Gross changes of salt volume through time were minimized by adjusted by broad warping of the sea floor and topography and the suprasalt blocks.

Full palinspastic restorations were made to 7 consecutive time steps. Any errors in the model stages that were revealed by subsequent restorations were corrected in the present-day model and all the intermediate restorations, so that the model was validated by 7 iterative steps.

Fig. 15: Marton et al. (2000) carried out the restoration of their Lower Congo Basin line using an unspecified software system. For the extensional domain, they used vertical slip (variable simple shear) to restore the fault blocks, and for the contractional domain they used flexural slip restoration. They did not apply decompaction.

Figs. 1 and 12: the Orange Basin line was constructed by the author from 2D seismic reflection data. The model was created as vectorgraphic polygons in CorelDraw. Restorations were carried out in the following stages: (i) translation (rigid block movement and rotation) to remove fault separation, (ii) deformation of the block to minimize fault gaps or overlaps. In contrast to the salt-floored system, the restored blocks were collaged in sequence from the bottom upwards, building up from the basal decollement. When all blocks are restored in this way, sea floor topography is obtained by construction. Any unreasonable irregularity in that topography was deemed to be the product of model error, and the model was amended to minimize this and re-restored. This was carried out iteratively until reasonable seafloor topography was obtained. No sediment decompaction was included in this restoration process.

References

Alsop, G.I., Marco, S., 2013. Seismogenic slump folds formed by gravity-driven tectonics down a negligible subaqueous slope. Tectonophysics 605, 48–69.

Bellahsen, N., Jolivet, L., Lacombe, O., Bellanger, M., Boutoux, A., Garcia, S., Mouthereau, F., Le Pourhiet, L., Gumiaux, C., 2012. Mechanisms of margin inversion in the external Western Alps: implications for crustal rheology. Tectonophysics 560, 62–83. http://dx.doi.org/10.1016/j.tecto.2012.06.022.

Benedicto, A., Séguret, M., Labaume, P., 1999. Interaction between faulting, drainage and sedimentation in extensional hangingwall syncline basins: example of the Oligocene Matelles basin (Gulf of Lion rifted margin, SE France). In: Durand, B., Jolivet, L., Horvath, F., Seranne, M. (Eds.), The Mediterranean Basins: Tertiary Extension within the Alpine Orogen. Geological Society, London, Special Publications, 156, pp. 81–108. http://dx.doi.org/10.1144/GSL.SP.1999.156.01.06.

Brown Jr., L.F., Benson, J.M., Brink, G.J., Doherty, S., Jollands, A., Jungslager, E.H.A., Keenan, J. H.G., Muntingh, A., Van Wyk, N.J.S., 1995. Sequence stratigraphy in offshore South African divergent basins—an atlas of exploration for Cretaceous lowstand traps by Soekor Ltd AAPG Stud. Geol. 41 (184 pp.).

Brun, J.-P., Fort, X., 2011. Salt tectonics at passive margins: geology versus models. Mar. Pet. Geol. 28, 1123–1145.

Brun, J.-P., Merle, O., 1985. Strain patterns in models of spreading–gliding nappes. Tectonics 4 (7), 705–719.

Bucher, W.H., 1956. Role of gravity in orogenesis. Geol. Soc. Am. Bull. 67, 1295–1318.

Burollet, P.F., 1975. Tectonique en radeaux en Angola (Raft tectonics in Angola). Bull. Soc. Geol. Fr. XVII, 503–504.

Butler, R.W.H., 1986. Thrust tectonics, deep structure and crustal subduction in the Alps and Himalayas. J. Geol. Soc. 143 (6), 857–873.

Butler, R.W.H., 2013. Area balancing as a test of models for the deep structure of mountain belts, with specific reference to the Alps. J. Struct. Geol. 52, 2–16.

Cruden, D.M., Varnes, D.J., 1996. Landslide types and processes. In: Turner, A.K., Shuster, R. L. (Eds.), Landslides: Investigation and Mitigation. Transp Res Board, Spec Rep, 247, pp. 36–75.

De Jong, K.A., Scholten, R., 1973. Preface. In: De Jong, K.A., Scholten, R. (Eds.), Gravity and Tectonics. John Wiley and Sons, New York, pp. ix–xviii.

De Vera, J., Granado, P., McClay, K., 2010. Structural evolution of the Orange Basin gravity-driven system, offshore Namibia. Mar. Pet. Geol. 27, 223–237.

Deville, E., Chauvière, A., 2000. Thrust tectonics at the front of the western Alps: constraints provided by the processing of seismic reflection data along the Chambéry transect. C. R. Acad. Sci. 331, 725–732.

Duval, B., Cramez, C., Jackson, M.P.A., 1992. Raft tectonics in the Kwanza Basin, Angola. Mar. Pet. Geol. 9, 389–404. http://dx.doi.org/10.1016/0264-8172(92)90050-O.

Elliott, D., 1976. The energy balance and deformation mechanisms of thrust sheets. Philos. Trans. R. Soc. London, Ser. A 283, 289–312.

Ellis, P.G., McClay, K.R., 1988. Listric extensional fault systems: results of analogue model experiments. Basin Res. 1, 55–70.

Fallot, P., Faure-Muret, A., 1949. Sur l'extension du decollement de la serie de couverture subalpine. CR Acad. Sci. Paris 228, 616–619.

Hudec, M.R., Jackson, M.P.A., 2002. Structural segmentation, inversion, and salt tectonics on a passive margin: evolution of the Inner Kwanza Basin, Angola. Geol. Soc. Am. Bull. 114, 1222–1244.
Hudec, M.R., Jackson, M.P.A., 2004. Regional restoration across the Kwanza Basin, Angola: salt tectonics triggered by repeated uplift of a metastable passive margin. AAPG Bull. 88, 971–990.
Jackson, M.P.A., Hudec, M.R., 2005. Stratigraphic record of translation down ramps in a passive-margin salt detachment. J. Struct. Geol. 27, 889–911.
Kehle, K.O., 1970. Analysis of gravity sliding and orogenic translation. Geol. Soc. Am. Bull. 81, 1641–1664.
Lundin, E., 1992. Thin-skinned extensional tectonics on a salt detachment, northern Kwanza Basin, Angola. Mar. Pet. Geol. 9, 405–411.
Marton, G., Tari, G., Lehmann, C., 1998. Evolution of salt-related structures and their impact on the post-salt petroleum systems of the Lower Congo Basin, offshore Angola. American Association of Petroleum Geologists International Conference and Exhibition, Rio de Janeiro. Extended Abstracts Volume, p. 834.
Marton, L.G., Tari, G.C., Lehmann, C.T., 2000. Evolution of the Angolan passive margin, West Africa, with emphasis on post-salt structural styles. In: Mohriak, W., Talwani, M. (Eds.), Atlantic Rifts and Continental Margins. American Geophysical Union Geophysical Monograph, 115, pp. 129–149.
Masson, D.G., Harbitz, C.B., Wynn, R.B., Pedersen, G., Løvholt, F., 2006. Submarine landslides: processes, triggers and hazard prediction. Phil. Trans. R. Soc. A 364. http://dx.doi.org/10.1098/rsta.2006.1810.
Mauduit, T., Guérin, G., Brun, J.-P., Lecanu, H., 1997. Raft tectonics: the effects of basal slope value and sedimentation rate on progressive extension. J. Struct. Geol. 19, 1219–1230.
Montgomery, D.R., Som, S.M., Jackson, M.P.A., Schreiber, B.S., Gillespie, A.G., Adams, J.B., 2009. Continental-scale salt tectonics on Mars and the origin of Valles Marineris and associated outflow channels. Geol. Soc. Am. Bull. 121 (1–2), 117–133. http://dx.doi.org/10.1130/B26307.1.
Moore, M.G., 2010. Exploration, appraisal, and development of turbidite reservoirs in the Western Atwater foldbelt. Deep Water Gulf of Mexico AAPG Annual Convention and Exhibition—11–14 April 2010.
Moretti, I., Wu, S., Bally, A., 1990. Computerized balanced cross section LOCACE to reconstruct an allochthonous salt sheet, offshore Louisiana. Mar. Pet. Geol. 7, 371–377.
Morley, C.K., King, R., Hillis, R., Tingay, M., Backe, G., 2011. Deepwater fold and thrust belt classification, tectonics, structure and hydrocarbon prospectivity: a review. Earth Sci. Rev. 104 (1–3), 41–91. http://dx.doi.org/10.1016/j.earscirev.2010.09.010 (January 2011).
Peel, F.J., Travis, C.J., Hossack, J.R., 1995. Genetic structural provinces and salt tectonics of the Cenozoic offshore US Gulf of Mexico: a preliminary analysis. In: Martin, M.P.A., Roberts, D.G., Snelson, S. (Eds.), Salt Tectonics: A Global Perspective. AAPG Memoir, 65, pp. 153–175.
Peel, F., Jackson, M., Ormerod, D., 1998. Influence of major steps in the base of salt on the structural style of overlying thin-skinned structures in deep water Angola. American Association of Petroleum Geologists International Conference and Exhibition, Rio de Janeiro, Brazil, November. Extended Abstracts Volume, pp. 366–367.
Phillippe, Y., Deville, E., Mascle, A., 1998. Thin-skinned inversion tectonics at oblique basin margins: example of the western Vercors and Chartreuse Subalpine massifs (SE France). In: Mascle, A., Puigdefabregas, C., Luterbacher, H.P., Fernandez, M. (Eds.), Cenozoic Foreland Basins of Western Europe Geological Society, Special Publications, 134, pp. 239–262.
Platt, J.P., 1986. Dynamics of orogenic wedges and the uplift of high-pressure metamorphic rocks. Geol. Soc. Am. Bull. 97, 1037–1053.
Ramberg, H., 1967. Gravity, Deformation and the Earth's Crust. Academic Press, London (217 pp.).
Ramberg, H., 1975. Particle paths, displacement and progressive strain applicable to rocks. Tectonophysics 28, 1–37.
Ramberg, H., 1977. Some Remarks on the Mechanism of Nappe Movement, Geol. Foremingen. Stockholm Forhandlingar, pp. 110–117.
Ramberg, H., 1981a. The role of gravity in orogenic belts. In: McClay, K.R., Price, N.J. (Eds.), Thrust and Nappe Tectonics. Special Publications of the Geological Society of London, 9, pp. 125–140.
Ramberg, H., 1981b. Gravity, Deformation and the Earth's Crust in Theory, Experiments and Geological Application, 2nd edition. Academic Press, London (452 pp.).
Rey, P., Vanderhaeghe, O., Teyssier, C., 2001. Gravitational collapse of the continental crust: definition, regimes and modes. Tectonophysics 342, 435–449.
Rowan, M.G., Trudgill, B.D., Fiduk, J.C., 2000. Deepwater, salt-cored fold belts: lessons from the Mississippi Fan and Perdido fold belts, northern Gulf of Mexico. In: Mohriak, W., Talwani, M. (Eds.), Atlantic Rifts and Continental Margins: American Geophysical Union Geophysical Monograph, 115, pp. 173–191.
Rowan, M.G., Peel, F.J., Vendeville, B.C., 2004. Gravity-driven fold belts on passive margins. In: McClay, K.R. (Ed.), Thrust Tectonics and Hydrocarbon Systems: AAPG Mem., 82, pp. 157–182.
Rowan, M.G., Peel, F.J., Vendeville, B.C., Gaullier, V., 2012. Salt tectonics at passive margins: geology versus models — discussion. Mar. Pet. Geol. 37, 184–194.
Schack Pedersen, S.A., 1987. Comparative studies of gravity tectonics in Quaternary sediments and sedimentary rocks related to fold belts. In: Jones, M.E., Preston, R.M.F. (Eds.), Deformation of Sediments and Sedimentary Rocks. Geological Society Special Publication, 29, pp. 165–180. http://dx.doi.org/10.1144/GSL.SP.1987.029.01.14.
Schultz-Ela, D., 2001. Excursus on gravity gliding and gravity spreading. J. Struct. Geol. 23, 725–731.
Stewart, S.A., 2011. Vertical exaggeration of reflection seismic data in geoscience publications 2006–2010. Mar. Pet. Geol. 28 (5), 959–965 (May 2011).
van Bemmelen, R.W., 1960. New views on East-Alpine orogenesis. Rep. 21st Int. Geol. Congr. Copenhagen, 18, pp. 99–116.
van Bemmelen, R.W., 1965. Tectogenèse par gravité. Ann. Soc. Geol. Belg. Bull. 64, 95–123.
Varnes, D.J., 1978. Slope movement types and processes. In: Schuster, R.L., Krizek, R.J. (Eds.), Landslides, Analysis and Control. Transportation Research Board Special Report No. 176, Nat. Acad. of Sciences, pp. 11–33.
Worrall, D.M., Snelson, S., 1989. Evolution of the northern Gulf of Mexico, with emphasis on Cenozoic growth faulting and the role of salt. In: Bally, A.W., Palmer, A.R. (Eds.), The Geology of North America: An Overview: Boulder, Colorado, Geological Society of America, Geology of North America, v. A, pp. 97–138.